Available online at www.sciencedirect.com

SCIENCE DIRECT®

Inorganica Chimica Acta 359 (2006) 1207–1214

Inorganica Chimica Acta

www.elsevier.com/locate/ica

Preparation, crystal structure and luminescent properties of the 3-D netlike supramolecular lanthanide picrate complexes with 2,2′-[1,2-phenylenebis(oxy)]bis(*N*-benzylacetamide)

Kuan-Zhen Tang [a], Jian Zhang [a], Yu Tang [a,*], Wei-Sheng Liu [a], Min-Yu Tan [a], Yu-Xi Sun [b]

[a] *College of Chemistry and Chemical Engineering, Lanzhou University, Lanzhou, Gansu 730000, PR China*
[b] *Department of Chemistry, Qufu Normal University, Qufu 273165, PR China*

Received 4 August 2005; received in revised form 6 October 2005; accepted 6 October 2005
Available online 8 November 2005

Abstract

Solid complexes of lanthanide picrates with a new podand-type ligand, 2,2′-[(1,2-phenylene)bis(oxy)]bis(*N*-benzylacetamide) (**L**) have been prepared and characterized by elemental analysis, conductivity measurements, IR, electronic and ^{1}H NMR spectroscopies. The crystal and molecular structures of the complex Nd**L**(Pic)$_3$ have been determined by single-crystal X-ray diffraction. The crystal structure shows that the Nd(III) ion is coordinated with four oxygen atoms of the ligand **L** and six oxygen atoms of three bidentate picrates. Furthermore, the Nd**L**(Pic)$_3$ complex units are linked by the intermolecular hydrogen bonds to form a three-dimensional (3-D) netlike supermolecule. Under excitation, Eu complex exhibited characteristic emissions. The lowest triplet state energy level of the ligand indicates that the triplet state energy level of the ligand matches better to the resonance level of Eu(III) than Tb(III) ion.

Keywords: Lanthanide picrate complexes; Podand; Crystal structure; Luminescent properties

1. Introduction

Many lanthanide complexes are noted for their luminescence arising from f–f transitions, which result in emission bands with extremely narrow bandwidth and no theoretical cap on the quantum efficiency [1]. This makes lanthanide ions very attractive for a variety of applications, such as chromophores for LEDs and as probes and labels in a variety of biological and chemical applications [2]. And the probes based on europium and terbium ions are of special interest because of the particularly suitable spectroscopic properties of these ions, such as their large Stokes shift and narrow emission profiles [1a,3]. Since the f–f transitions are spin- and parity-forbidden, the excited state of the lanthanide ion is populated through intramolecular energy transfer from the ligand or ligands, which therefore serve as sensitizers (antenna effect) [4]. The role of the ligands is on one hand to collect the photons provided by the light source in order to allow an energy transfer to the energy levels of the Ln(III) ion, and on the other hand to shield it against the solvent in order to avoid non-radioactive deactivation processes. It is generally accepted that the energy transfer from ligand to Ln(III) ion occurs from the lowest triplet state energy level (T$_1$) of the ligand to the resonance level of Ln(III) [5]. This energy transfer process is one of the most important processes having influence on the luminescence properties of the lanthanide complexes. Podand-type ligands have drawn much attention in recent years, mainly due to their selective coordinating capacity and hard binding sites, therefore, stabilizing their complexes, acquiring novel coordination structure and shielding the encapsulated ion from interaction with the surroundings [6]. Among numerous podands which have demonstrated their potential use in functional supramolecular chemistry [7], amide type podands are important for

---

[*] Corresponding author. Tel.: +869318912552; fax: +869318912582.
E-mail address: tangyu@lzu.edu.cn (Y. Tang).

0020-1693/$ - see front matter © 2005 Elsevier B.V. All rights reserved.
doi:10.1016/j.ica.2005.10.004

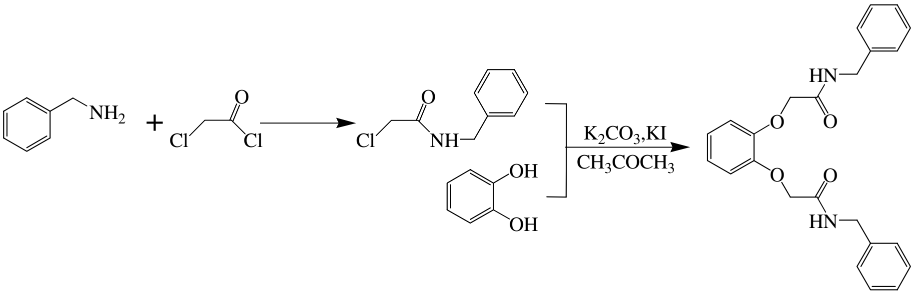

Scheme 1. The synthetic route for the ligand **L**.

preparing the lanthanide complexes possessing strong luminescent properties.

Our group is interested in the supramolecular coordination chemistry of lanthanide ions with amide type podands that have strong coordination capability to the lanthanide ions and terminal group effects [8]. We have designed a series of amide type podands having both selective ability to coordinate lanthanide ions and enhanced luminescence of lanthanide complexes by providing some of proper conjugate absorption groups suitable for energy transfer [9]. In the present work, we designed and synthesized a new amide type podand ligand 2,2′-[(1,2-phenylene)bis(oxy)]bis(*N*-benzylacetamide) (**L**) (Scheme 1) with two relatively long "arms", and studied the crystal structure and luminescent properties of lanthanide complexes with this new ligand. The crystal structure of the complex Nd**L**(Pic)$_3$ shows that the Nd(III) ion could be effectively encapsulated and protected by the coordinated ligands. And the two nitrogen atoms of the amide groups in the ligand arms are located in the outer part of the whole ligand molecule, which is very important for the assembly of the complex molecule units into a three-dimensional (3-D) netlike supermolecule by the intermolecular hydrogen bonds. Under excitation, Eu complex exhibited characteristic emissions. And the lowest triplet state energy level of the ligand which was calculated from the phosphorescence spectrum of the Gd complex at 77 K indicates that the triplet state energy level of the ligand matches better to the resonance level of Eu(III) than Tb(III) ion.

2. Experimental

2.1. Materials

Lanthanide picrates [10] and chloracetobenzylamine [11] were prepared according to the literature methods. Other chemicals were obtained from commercial sources and used without further purification.

2.2. Preparation of the ligand L

The synthetic route for the ligand is shown in Scheme 1. Chloracetobenzylamine (0.96 g, 8.73 mmol) and *o*-dihydroxybenzene (3.2 g, 17.44 mmol) were added to acetone (25 cm^3), then anhydrous potassium carbonate (2.4 g, 17.40 mmol) and a small quantity of KI were added. The reaction mixture was stirred and refluxed for 5 h. After cooling down, the mixture was filtered and the solvent was distilled off. Then the resulted solid was recrystallized with acetone to get the ligand **L**; Yield: 75%. m.p. 114–115 °C; ^{1}H NMR (CDCl$_3$, 300 MHz) δ: 4.42 (d, $J = 6.0$ Hz, 4H), 4.50 (s, 4H), 6.96 (s, 2H), 6.88–7.03 (m, 4H), 7.17–7.31 (m, 10H); *Anal.* Calc. for $C_{24}H_{24}N_2O_4$: C, 71.27; H, 5.98; N, 6.93. Found: C, 70.94; H, 5.90; N, 7.09%.

2.3. Preparation of the complexes

A solution of 0.1 mmol **L** in 10 cm^3 of ethyl acetate was added drop wise to a solution of 0.1 mmol lanthanide picrates (Ln = La, Pr, Nd, Eu, Gd, Tb, Er) in 10 cm^3 of ethyl acetate. The mixture was stirred at room temperature for 4 h. Then diethyl ether was added to the mixture and the precipitated solid complex was filtered, washed with ethyl acetate and diethyl ether and dried in vacuo over P_4O_{10} for 48 h and submitted for elemental analysis; Yield: 60%. Analytical data and molar conductance values of the complexes are given in Table 1. All the complexes are yellow powders and stable in air. Single crystals of neodymium complex were grown from ethyl acetate and chloroform (V:V = 1:3) mixed solution with slow evaporation at room temperature. After ca. 3 weeks, transparent yellow crystals were formed from the solution.

2.4. Chemical and physical measurements

The Ln(III) ion was determined by EDTA titration using xylenol-orange as an indicator. Carbon, nitrogen and hydrogen were determined using an Elementar Vario EL (see Table 1). The IR spectra were recorded in the 4000–400 cm^{-1} region using KBr pellets and a Nicolet Nexus 670 FT-IR spectrometer (see Table 4). ^{1}H NMR spectra were measured on a Varian Mercury 300 spectrometer in CDCl$_3$ and CD$_3$COCD$_3$ solutions, with TMS as internal standard. Electronic spectra were recorded with a Varian Cary 100 spectrophotometer in acetonitrile solution. Luminescence spectra and phosphorescence spectra were obtained on a Hitachi F-4500 fluorescence spectrophotometer.

Table 1
Analytical and molar conductance data of the complexes (calculated values in parentheses)

Complexes	%C Found (Calc.)	%H Found (Calc.)	%N Found (Calc.)	%Ln Found (Calc.)	Λ_m (cm^2 Ω^{-1} mol^{-1})
La**L**(Pic)$_3$	41.35 (41.09)	2.35 (2.46)	12.88 (12.55)	11.50 (11.31)	50.2[a], 35.5[b]
Pr**L**(Pic)$_3$	41.22 (41.02)	2.20 (2.46)	12.95 (12.53)	11.75 (11.46)	51.5[a], 37.0[b]
Nd**L**(Pic)$_3$	41.34 (40.91)	2.30 (2.45)	12.85 (12.50)	11.90 (11.70)	50.6[a], 32.7[b]
Eu**L**(Pic)$_3$	40.98 (40.66)	2.25 (2.44)	12.75 (12.42)	11.99 (12.25)	50.9[a], 33.9[b]
Gd**L**(Pic)$_3$	40.85 (40.49)	2.30 (2.43)	12.12 (12.37)	12.38 (12.62)	52.5[a], 38.3[b]
Tb**L**(Pic)$_3$	40.72 (40.43)	2.22 (2.42)	12.55 (12.35)	12.56 (12.74)	50.4[a], 32.8[b]
Er**L**(Pic)$_3$	40.74 (40.16)	2.35 (2.41)	12.60 (12.27)	13.01 (13.32)	52.8[a], 33.6[b]

[a] Measured in acetonitrile.

[b] Measured in acetone.

2.5. Crystal structure determination

X-ray diffraction data for a crystal of the neodymium complex with dimensions 0.14 × 0.13 × 0.08 mm were performed with graphite-monochromated Mo Kα radiation on a Bruker APEX area-detector diffractometer and were collected by the ω–2θ scan technique. The crystal structures were solved by direct methods. All non-hydrogen atoms were refined anisotropically by full-matrix least-squares methods on F^2. Primary non-hydrogen atoms were solved by direct method and secondary non-hydrogen atoms were solved by difference maps. The hydrogen atoms were added geometrically and not refined. All calculations were performed using the programs SHELXS-97 and SHELXL-97 [12,13] (see Table 2). Selected bond lengths and angles are presented in Table 3. The complex Nd**L**(Pic)$_3$ crystallizes in the monoclinic system, space group $P2_1/a$, with lattice parameters $a = 12.293(14)$ Å, $b = 34.259(4)$ Å, $c = 12.298(14)$ Å, $\beta = 112.710(2)°$, $F(000) = 2476$, GOF = 1.019, $R_1 = 0.0555$, $wR_2 = 0.1078$, $Z = 4$. $\rho_{calc} = 1.714$ g cm^{-3}, $V = 4777.6(9)$ Å^3, $\lambda = 0.71073$ Å, $T = 295$ K.

Table 2
Crystal data and structure refinement for the complex Nd**L**(Pic)$_3$

Complex	Nd**L**(Pic)$_3$
Empirical formula	$C_{42}H_{30}N_{11}O_{25}Nd$
Formula weight	1233.01
Colour	yellow
Temperature (K)	295(2)
Wavelength (Å)	0.71073
Radiation	Mo Kα
Crystal system	monoclinic
Space group	$P21/a$
Unit cell dimensions	
a (Å)	12.293(14)
b (Å)	34.259(4)
c (Å)	12.298(14)
β (°)	112.710(2)
Volume (Å^3)	4777.6(9)
Z	4
D_{calc} (g cm^{-3})	1.714
μ (Mo Kα) (mm^{-1})	1.191
$F(000)$	2476
Crystal size (mm)	0.14 × 0.13 × 0.08
Range (°)	1.19–25.50
Index ranges	$-14 \leqslant h \leqslant 14$; $-41 \leqslant k \leqslant 40$; $-14 \leqslant l \leqslant 14$
Reflection collected	8871
Independent reflections (R_{int})	5919 (0.0918)
Absorption correction	multi-scan
Refinement method	full-matrix least-squares on F^2
Data/restraints/parameters	8871/162/700
Goodness-of-fit on F^2	1.019
Final R indices	$R_1 = 0.0555$, $wR_2 = 0.1078$
Largest difference peak and hole (e Å^{-3})	0.811 and −0.771

3. Results and discussion

Analytical data for the newly synthesized complexes, listed in Table 1, indicate that the seven picrates complexes conform to a 1:1:3 metal-to-ligand-to-picrate stoichiometry Ln**L**(Pic)$_3$ (Ln = La, Pr, Nd, Eu, Gd, Tb, Er).

All the complexes are soluble in DMF, DMSO, methanol, ethanol, acetonitrile, ethyl acetate and acetone, but slightly soluble in THF and CHCl$_3$. The molar conductances of the complexes in acetonitrile and acetone (see Table 1) indicate that all complexes act as non-electrolytes [14], implying that all picrates groups are in coordination sphere.

3.1. Crystal structure of Nd **L**(Pic)$_3$

A summary of crystallographic data and details of the structure refinements are listed in Table 2. The selected bond lengths and bond angles are given in Table 3.

The single-crystal X-ray analysis of the complex Nd**L**(Pic)$_3$ reveals that each Nd atom is coordinated with 10 oxygen donor atoms. Six of them belong to three bidentate picrate groups and the remaining four are from the tetradentate ligand **L** (Fig. 1). The coordination polyhedron around Nd is a distorted bicapped square antiprism (Fig. 2). The ligand wraps around the metal ion with its oxygen atoms and forms a ring-like coordination structure [15] together with the Nd atom. The four oxygen atoms of the ligand (O(1), O(2), O(3), O(4)) are not quite coplanar, their deviation from the mean plane being in the range 0.067–0.121 Å. The mean absolute deviation is 0.0935 Å from the mean plane. The neodymium atom lies out of this plane by 0.795 Å. The Nd–O (C=O) distances (mean 2.426 Å) are significantly shorter than the Nd–O (C–O–C) distances (mean 2.719 Å). This suggests that the Nd–O (C=O) bond is stronger than the Nd–O (C–O–C) bond.

Table 3
Selected bond lengths (Å) and angles (°) for the complex NdL(Pic)$_3$

Nd1–O1	2.438(5)	Nd1–O2	2.662(5)	Nd–O3	2.776(5)
Nd1–O4	2.415(5)	Nd1–O5	2.357(5)	Nd1–O6	2.594(5)
Nd1–O12	2.304(5)	Nd1–O13	2.843(6)	Nd1–O19	2.379(5)
Nd1–O20	2.674(6)				
O1–Nd1–O2	60.70(16)	O1–Nd1–O3	110.84(15)	O1–Nd1–O4	141.40(18)
O1–Nd1–O5	81.76(18)	O1–Nd1–O6	68.10(18)	O1–Nd1–O12	126.38(18)
O1–Nd1–O13	65.95(17)	O1–Nd1–O19	121.06(17)	O1–Nd1–O20	69.42(17)
O2–Nd1–O3	55.96(14)	O2–Nd1–O4	113.78(16)	O2–Nd1–O5	128.55(16)
O2–Nd1–O6	68.12(16)	O2–Nd1–O12	146.04(18)	O2–Nd1–O13	119.78(16)
O2–Nd1–O19	74.10(16)	O2–Nd1–O20	73.74(17)	O3–Nd1–O4	59.25(15)
O3–Nd1–O5	118.72(15)	O3–Nd1–O6	65.33(16)	O3–Nd1–O12	121.26(17)
O3–Nd1–O13	175.58(15)	O3–Nd1–O19	63.61(15)	O3–Nd1–O20	113.46(16)
O4–Nd1–O5	74.07(18)	O4–Nd1–O6	74.60(18)	O4–Nd1–O12	80.98(19)
O4–Nd1–O13	125.17(17)	O4–Nd1–O19	89.43(18)	O4–Nd1–O20	148.89(17)
O5–Nd1–O6	65.69(17)	O5–Nd1–O12	84.12(19)	O5–Nd1–O13	64.43(18)
O5–Nd1–O19	155.80(18)	O5–Nd1–O20	126.51(18)	O6–Nd1–O12	145.20(19)
O6–Nd1–O13	114.97(18)	O6–Nd1–O19	127.52(17)	O6–Nd1–O20	132.75(18)
O12–Nd1–O13	61.28(18)	O12–Nd1–O19	75.74(19)	O12–Nd1–O20	78.84(19)
O13–Nd1–O19	114.99(17)	O13–Nd1–O20	62.86(18)	O19–Nd1–O20	62.78(17)

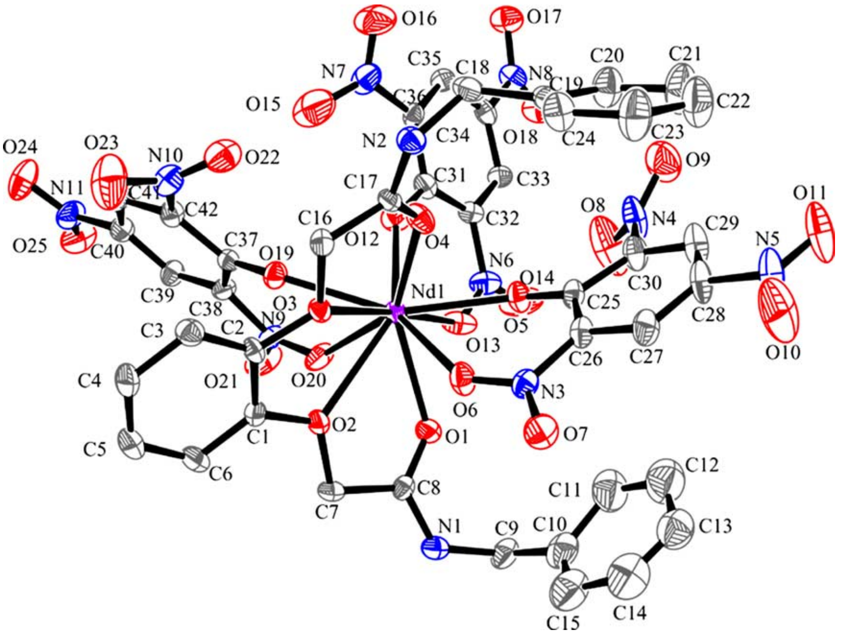

Fig. 1. ORTEP diagram (30% probability ellipsoids) showing the coordination sphere of NdL(Pic)$_3$.

In the complex, requirement of high coordination number of the lanthanide ion is satisfied by the tetradentate ligand and three bidentate picrate groups. Since coordinated solvent molecules, especially water or alcohol, can efficiently quench lanthanide luminescence, the ability of the ligands to satisfy the coordination requirements of the Ln(III) centre with high coordination number becomes an important criterion in the design of supramolecular photonic devices [16].

The conformation of the ligand **L** in the complex is interesting. The two arms of the ligand are so long that their terminal groups can "fold back". Through intramolecular π–π interaction [17], two benzyl groups of the two arms wrap around a coordinated picrate, one above and the other below, forming the "folding-shape" of the ligand (Fig. 3). These three almost parallel phenyl rings are separated by 3.808 Å (*a* and *b*) and 3.051 Å (*a* and *c*) (vertical distance) and the dihedral angle between *a* and *b* is 27.2° and between *a* and *c* is 12.0°. Thus, the two nitrogen atoms of the amide groups in the ligand, namely, N(1) and N(2), are located in the outer part of the whole ligand molecule (Fig. 3), which is very important for the assembly of the complex molecule units into the supermolecule by the intermolecular hydrogen bonds.

In the complex, atoms N(1) and N(2) of the ligand **L** act as hydrogen bond donors to form O···H–N with the oxygen atoms O(14), O(16) and O(18) of a neighbouring

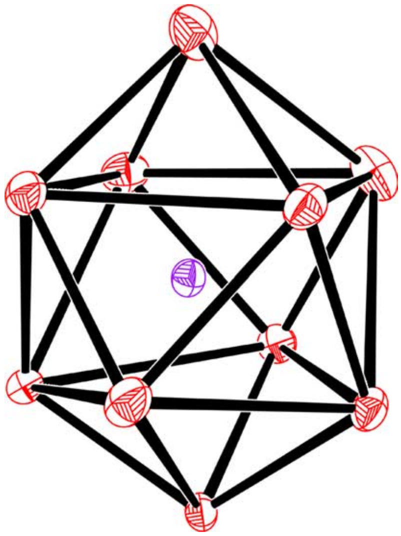

Fig. 2. Coordination polyhedron of Nd ion.

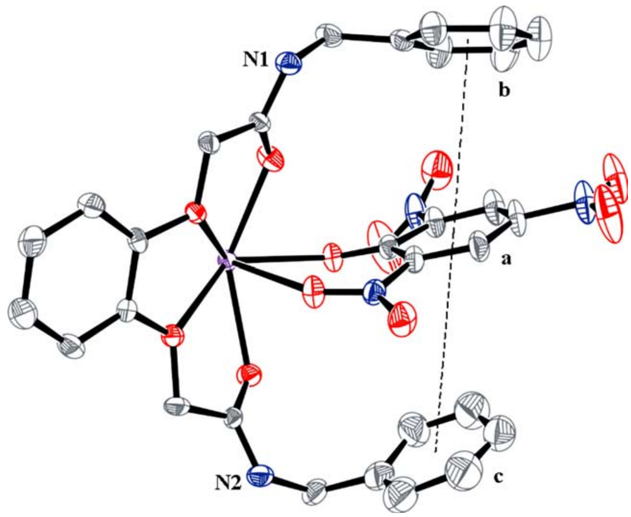

Fig. 3. The intramolecular π–π stacking interactions in the complex molecule.

molecule [O(14)···H(1), 2.09 Å and O(14)···H(1)–N(1), 168°; O(16)···H(2), 2.46 Å, O(18)···H(2), 2.57 Å and O(16)···H(2)–N(2), 149°, O(18)···H(2)–N(2), 135°], thus, generating a two-dimensional (2-D) supramolecular layer as shown in Fig. 4(a). In addition, the layers are linked by intermolecular hydrogen bond O(7)···H(39)–C(39) [O(7)···H(39), 2.59 Å and O(7)···H(39)–C(39), 170°] [18] as shown in Fig. 4(b) to form a three-dimensional (3-D) netlike supermolecule.

3.2. Infrared spectra

The most important IR peaks of the ligand and the complexes Ln**L**(Pic)$_3$ are reported in Table 4.

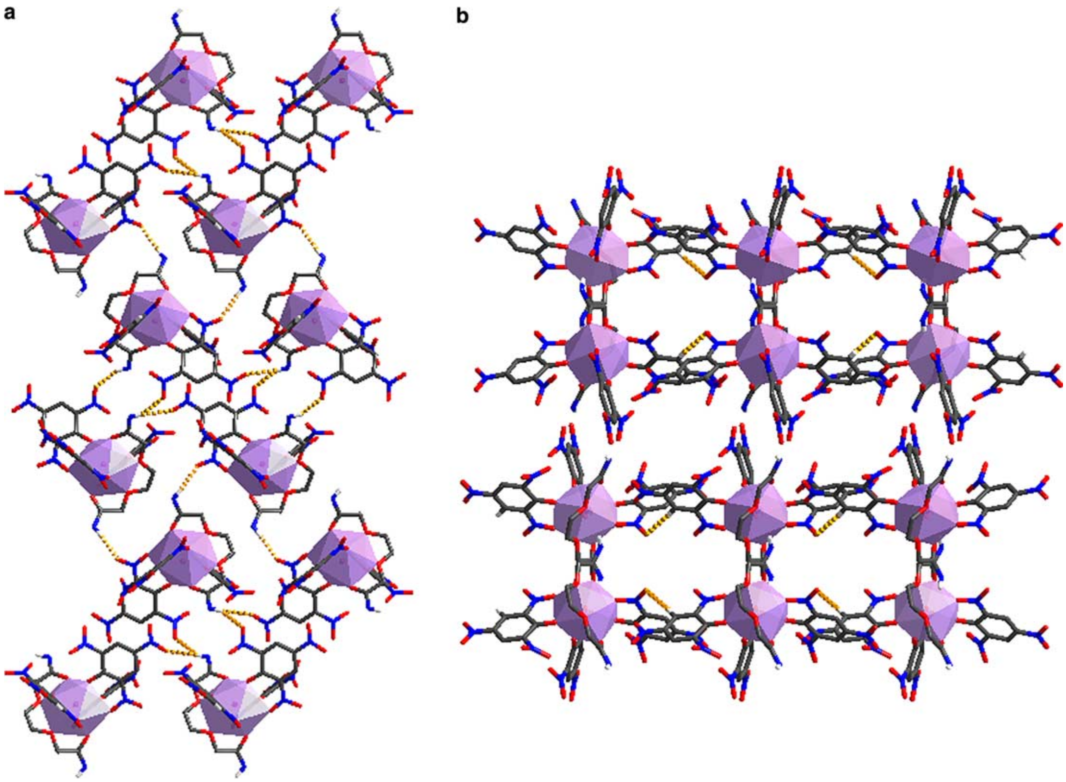

Fig. 4. Hydrogen bonding networks in the complexes: (a) 2-D layers generated by the intermolecular O···H–N hydrogen bonds [symmetry codes for O(14)···H(1)–N(1), O(16)···H(2)–N(2) and O(18)···H(2)–N(2) are: $-1/2 + x$, $1/2 - y$, z; $1 - x$, $-y$, $1 - z$; and $-1 + x$, y, z, respectively]; (b) The intermolecular O···H–C hydrogen bonds [symmetry code is x, y, $-1 + z$] between the 2-D layers (some atoms of the ligand are omitted for clarity and the hydrogen bonds are indicated by the yellow dashed lines).

Table 4
The IR spectra data (cm^{-1})

Compounds	v(C=O)	v(C–O–C)	v(C–O)	v_{as}($-NO_2$)	v_s($-NO_2$)
HPic			1265s	1555m	1342s
L	1660s	1053m			
La**L**(Pic)$_3$	1616s	1020m	1271m	1574m, 1541m	1362m, 1331m
Pr**L**(Pic)$_3$	1616s	1018m	1272m	1570m, 1543m	1362m, 1334m
Nd**L**(Pic)$_3$	1615s	1020m	1270m	1577m, 1542m	1361m, 1331m
Eu**L**(Pic)$_3$	1617s	1024m	1272m	1574m, 1542m	1360m, 1334m
Gd**L**(Pic)$_3$	1616s	1017m	1271m	1573m, 1544m	1362m, 1333m
Tb**L**(Pic)$_3$	1617s	1021m	1270m	1575m, 1540m	1357m, 1331m
Er**L**(Pic)$_3$	1617s	1020m	1270m	1576m, 1540m	1362m, 1333m

The "free" ligand **L** exhibit two absorption bands at 1660 and 1053 cm^{-1} which are assigned to v(C=O) and v(C–O–C), respectively. In the complexes, the bonds shift by ca. 45 and 30 cm^{-1} towards lower wave numbers, thus indicating that the C=O and ether O-atoms take part in coordination to the metal ions. The larger shifts v(C=O) in the spectra of the complexes suggest that the Ln–O (carbonyl) bond is stronger than the Ln–O (ether) bond. And this is in agreement with the crystal structure analysis.

The OH out-of-plane bending vibration of the free HPic at 1151 cm^{-1} disappears, indicating that the H-atom of the OH group is replaced by Ln(III). The vibration v(C–O) of Pic^- at 1265 cm^{-1} is shifted toward higher frequency by ca. 5 cm^{-1} in the complexes. This is due to the following two effects. First, the hydrogen atom of the OH group is replaced by Ln(III), increasing the π-bond character in the C–O bond. Secondly, coordination of the oxygen atom of **L** to Ln(III) decreases the π-character. The free HPic has v_{as}($-NO_2$) and v_s($-NO_2$) at 1555 and 1342 cm^{-1}, respectively, which split into two bands at ca. 1575, 1542 cm^{-1} and ca. 1360, 1330 cm^{-1}, respectively, in the complexes. This indicates that O-atoms in the nitro group of Pic^- take part in coordination [19]. On the basis of the similarity of their IR spectra, it may be assumed that the complexes have the similar structures.

3.3. ^1H NMR spectra

The ^1H NMR spectra of the "free" ligand **L** and the diamagnetic Ln(III) complex La**L**(Pic)$_3$ were measured in CD_3COCD_3. Owing to the solvent effect, the ^1H NMR spectrum of free **L** in CD_3COCD_3 is slightly different from that in $CDCl_3$ (vide ante). In CD_3COCD_3, the spectrum of **L** exhibits two unsolved multiplets at ca. 7.25 and 7.01 ppm, a singlet at 4.59 and a doublet at 4.43 ppm ($J = 6$ Hz), assigned to $-C_6H_5-$, $-C_6H_4-$, –C(O)–CH_2–, –N–CH_2–, respectively. Upon coordination, the signal of –C(O)–CH_2– is shifted by 0.15 ppm and those of $-C_6H_4-$ protons by only 0.03 ppm. This is probably due to the inductive effect of Ln–O(**L**) bonds and a change in the conformation of the ligand in the complexes. The larger shift for –C(O)–CH_2– protons than for $-C_6H_4-$ protons indicates that the Ln–O(C=O) bond is stronger than the Ln–O(C–O–C) bond.

The ^1H signal of the OH group in the free HPic disappears in the complex, indicating that the H-atom of the OH group is replaced by Ln(III). The benzene ring protons of the free HPic exhibit a singlet at 9.12 ppm. Upon coordination, the signal moves to higher field. Only one singlet is observed for the benzene ring protons of the three coordination picrate groups, indicating fast exchange among the groups in solution [20].

3.4. Electronic spectra

The electronic spectra in the visible region of the Ln(III) complexes exhibit alternations in intensity and shifts in position of the absorption bands relative to the corresponding Ln(III) aquo ions. The shift has been attributed by Jørgensen to the effect on the crystal field of interelectronic repulsion between the 4f electrons, and is related to the covalent character of the metal–ligand bond, assessed by Sinha's parameter (δ), the nephelauxetic ration (β) and the bonding parameter ($b^{1/2}$) [21]. Absorption spectra of the Nd(III) complex was registered in acetonitrile solution at room temperature and the covalent parameters were calculated (Table 5). The values of β, which are less than unity, and positive values of δ and $b^{1/2}$ indicate that the metal–ligand bonds present some covalent character [22].

3.5. Luminescence properties of the complexes

Monitored by the emission band at 610 nm, Eu**L**(Pic)$_3$ exhibits broad excitation bands around 400 nm. The luminescence emission spectra of the ligand **L** and Eu**L**(Pic)$_3$ in solid state (the excitation and emission slit widths were 2.5 nm, Fig. 5(a)) and in ethyl acetate, acetone, acetonitrile, ethanol and methanol solutions (concentration: 1.0 ×

Table 5
Electronic spectral data and covalent parameters of Nd complex

Complex	Frequency (cm^{-1})	Assignment	Covalent parameters
Nd**L**(Pic)$_3$	19048	$^4I_{9/2} \rightarrow {}^4G_{9/2}$	$\beta = 0.9924$
	17212	$\rightarrow {}^2G_{7/2}$	$\delta = 0.7658$
	13405	$\rightarrow {}^4S_{3/2}$	$b^{1/2} = 0.06164$
	12484	$\rightarrow {}^2H_{9/2}$	

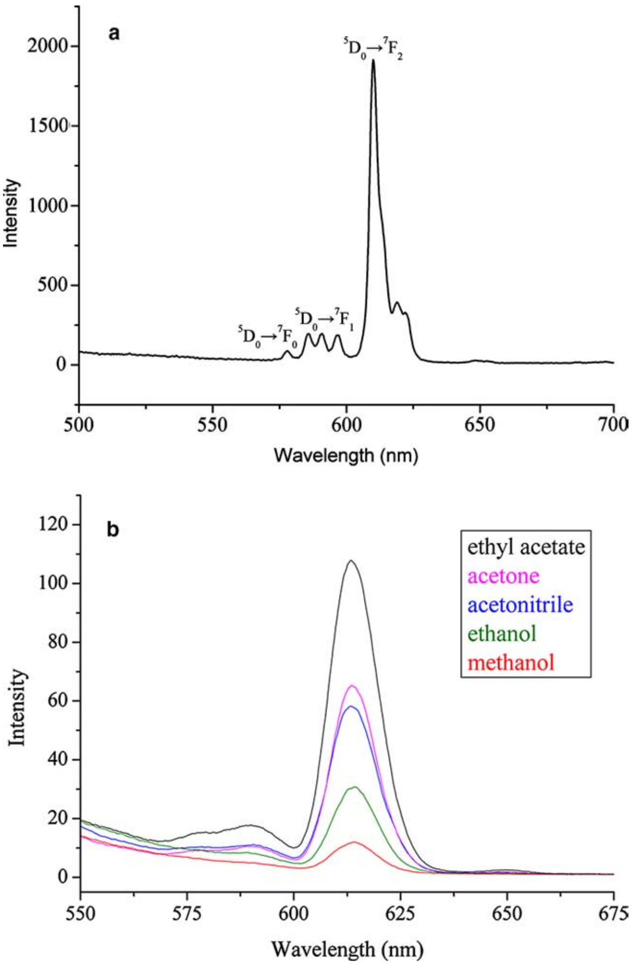

Fig. 5. Emission spectra of the Eu complex: (a) solid state; (b) in different solutions at room temperature.

10^{-3} mol L^{-1}, the excitation and emission slit widths were 5.0 nm, Fig. 5(b)) were recorded at room temperature. It can be seen from Fig. 5(a) that the Eu complex shows strong emission when excited with 400 nm in the solid state. This indicates that the ligand **L** is a comparative good organic chelator to absorb energy and transfer them to Eu ion. The most intensity ratio value $\eta(^5D_0 \to {}^7F_2/^5D_0 \to {}^7F_1)$ is 9.9, showing that the Eu(III) ion does not lie in a centro-symmetric coordination site [23], in agreement with the crystal structure analysis.

An intramolecular energy transfer from the triplet state of the ligand to the resonance level of the Ln(III) ion is one of the most important processes having influence on the Ln(III) luminescence properties of Ln(III) chelates [5b]. A triplet excited state T_1 which is localized on one ligand only and is independent of the lanthanide nature [5b]. In order to acquire the triplet excited state T_1 of the ligand **L**, the phosphorescence spectrum of the Gd(III) complex was measured at 77 K in a methanol–ethanol mixture (V:V = 1:1). The triplet state energy level T_1 of the ligand **L**, which was calculated from the shortest-wavelength phosphorescence band [5a], is 21 880 cm^{-1}. This energy level is above the lowest excited resonance level $^5D_0$ of Eu(III) (17 331 cm^{-1}) and $^5D_4$ (20 500 cm^{-1}) of Tb(III). Thus, the absorbed energy could be transferred from ligand to the Eu or Tb ions. And we may deduce that the triplet state energy level T_1 of this ligand **L** matches better to the lowest resonance level of Eu(III) ($\Delta v = 4549\ cm^{-1}$) than Tb(III) ($\Delta v = 1380\ cm^{-1}$) ion, because such small Δv (T_1–$^5D_4$) could result in the non-radioactive deactivation of the terbium emitting state via a back-energy transfer process ($T_1 \leftarrow Tb(^5D_4)$) and quench the luminescence of the Tb complex [5c]. Actually, we do not observe the luminescence of the Tb complex at room temperature in solid state or in solutions.

It could be seen from Fig. 5(b) that in ethyl acetate solution the Eu complex has the strongest luminescence, and then in acetone, acetonitrile, ethanol and methanol. This is due to the coordinating effects of solvents, namely solvate effect [24]. Together with the raising coordination abilities of ethyl acetate, acetone, acetonitrile, ethanol and methanol for the lanthanide ions, the oscillatory motions of the entering molecules consume more energy which the ligand triplet level transfer to the emitting level of the lanthanide ion. Thus, the energy transfer could not be carried out perfectly.

4. Conclusions

In summary, seven new lanthanide picrate complexes Ln**L**(Pic)$_3$ (Ln = La, Pr, Nd, Eu, Gd, Tb, Er) of a amide type podand ligand 2,2′-[(1,2-phenylene)bis(oxy)]bis(*N*-benzylacetamide) (**L**) were obtained and structurally characterized. The crystal structure of the complex Nd**L**(Pic)$_3$ shows that the Nd(III) ion is coordinated with four oxygen atoms of the ligand **L** and six oxygen atoms of three bidentate picrates. The two arms of the ligand are so long that their terminal groups can "fold back". Thus, the two nitrogen atoms of the amide groups in the ligand are located in the outer part of the whole ligand molecule, which is very important for the assembly of the complex molecule units into the supermolecule by the intermolecular hydrogen bonds. It is noteworthy that the ligand shield Ln^{3+} using its two long arms, thus, the solid Eu complex does possess comparatively strong luminescence at room temperature. And the lowest triplet state energy level of the ligand indicates that the triplet state energy level of the ligand matches better to the resonance level of Eu(III). To sum up, we designed a new podand ligand with two long arms, which can strongly bind Ln(III) ions to form elegant supramolecular architecture and sensitize Eu(III) emission.

5. Supplementary data

Crystallographic data for the structure reported in this paper have deposited with the Cambridge Crystallographic Data Centre and allocated the deposition number CCDC 279698. Copies of the data can be obtained free of charge on application to CCDC, 12 Union Road, Cambridge

CB2 1EZ, UK (fax: +44 1223 336 033; e-mail: deposit@ccdc.cam.ac.uk or http://www.ccdc.cam.ac.uk).

Acknowledgements

This work was supported by the National Natural Science Foundation of China (Project 20401008) and the Research Foundation for the Young Teachers Possessing Doctor's Degree of Lanzhou University.

References

[1] (a) F.S. Richardson, Chem. Rev. 82 (1982) 541;
(b) D. Parker, J.A.G. Williams, J. Chem. Soc., Dalton Trans. (1996) 3613.
[2] (a) J.F. Desreux, in: G.R. Choppin, J.-C. Bünzli (Eds.), Lanthanide Probes in Life, Chemical and Earth Sciences, Elsevier, Amsterdan, 1989;
(b) J.-C.G. Bünzli, C. Piguet, Chem. Rev. 102 (2002) 1897.
[3] I. Hemmilä, T. Stahlberg, P. Mottram, Bioanalytial Applications of Labelling Technologies, Wallac Oy, Turku, 1995.
[4] (a) G.F. Desa, O.L. Malta, C. De Mello Donega, A.M. Simas, R.L. Longo, P.A. Santa-cruz, E.F. da Silva Jr., Coord. Chem. Rev. 196 (2000) 165;
(b) C. Bazzicalupi, A. Bencini, A. Bianchi, C. Ciorgi, V. Fusi, A. Masotti, B. Valtancoli, A. Roque, F. Pina, Chem. Commun. 7 (2000) 561.
[5] (a) W. Dawson, J. Kropp, M. Windsor, J. Chem. Phys. 45 (1966) 2410;
(b) M. Latva, H. Takalob, V.-M. Mukkala, C. Matachescuc, J.C. Rodriguez-Ubisd, J. Kankarea, J. Luminesc. 75 (1997) 149;
(c) F. Gutierrez, C. Tedeschi, L. Maron, J.-P. Daudey, R. Poteau, J. Azema, P. Tisnès, C. Picard, J. Chem. Soc., Dalton Trans. (2004) 1334.
[6] (a) F. Renaud, C. Piguet, G. Bernardinelli, J.-C.G. Bunzli, G. Hopfgartner, J. Am. Chem. Soc. 121 (1999) 9326;
(b) L.H. Gade, Acc. Chem. Res. 35 (2002) 575;
(c) C.S. Hamann, A.V. Zelewsky, A. Barbieri, F. Barigelletti, G. Muller, J.P. Riehl, A. Neels, J. Am. Chem. Soc. 126 (2004) 9339.
[7] (a) C.Y. Su, Y.P. Cai, C.L. Chen, M.D. Smith, W. Kaim, H.C. zur Loye, J. Am. Chem. Soc. 125 (2003) 8595;
(b) C.Y. Su, Y.P. Cai, C.L. Chen, F. Lissner, B.S. Kang, W. Kaim, Angew. Chem., Int. Ed. Engl. 41 (2002) 3371.
[8] B. Tümmler, G. Maass, F. Vögtle, J. Am. Chem. Soc. 101 (1979) 2588.
[9] (a) J. Zhang, Y. Tang, N. Tang, M.Y. Tan, W.S. Liu, K.B. Yu, J. Chem. Soc., Dalton Trans. (2002) 832;
(b) Z.H. Cai, Y. Tang, W.S. Liu, M.Y. Tan, Chem. Lett. 3 (2004) 342;
(c) Y. Tang, J. Zhang, W.S. Liu, M.Y. Tan, K.B. Yu, Polyhedron 24 (2005) 1160.
[10] Y.C. Tian, Y.Q. Liang, J.Z. Ni, Chin. Univ. Chem. J. 9 (1988) 113.
[11] W. Baker, K.M. Buggle, J.F.W. McOmie, D.A.M. Watkins, J. Chem. Soc. (1958) 3594.
[12] G.M. Sheldrick, Acta Crystallogr. A46 (1990) 467.
[13] G.M. Sheldrick, SHELXS-97, A Program for X-ray Crystal Structure Solution, and SHELXL-97, A Program for X-ray Structure Refinement, Gottingen University, Germany, 1997.
[14] W.J. Geary, Coord. Chem. Rev. 7 (1971) 81.
[15] L.Y. Fan, W.S. Liu, X.M. Gan, N. Tang, M.Y. Tan, W.H. Jiang, K.B. Yu, Polyhedron 19 (2000) 779.
[16] N. Sabbatini, M. Guardigli, J.M. Lehn, Coord. Chem. Rev. 123 (1993) 201.
[17] C. Janiak, J. Chem. Soc., Dalton Trans. (2000) 3885.
[18] G.R. Desiraju, Acc. Chem. Res. 29 (1996) 441.
[19] S.X. Liu, W.S. Liu, M.Y. Tan, K.B. Yu, J. Coord. Chem. 10 (1996) 391.
[20] X. Mao, L.F. Shen, J.Z. Ni, Bopuxuezazhi 1 (1985) 201.
[21] (a) C.K. Jørgenson, Prog. Inorg. Chem. 4 (1962) 73;
(b) S.P. Sinha, Spectrochim. Acta 22 (1966) 57;
(c) D.E. Henrie, G.R. Choppin, J. Chem. Phys. 49 (1968) 477.
[22] A.K. Solanki, A.M. Bhandaka, J. Inorg. Nucl. Chem. 41 (1979) 1311.
[23] M. Albin, R.R. Wright Jr., W.D. Horrocks, Inorg. Chem. 24 (1985) 2491.
[24] H.Q. Liu, T.C. Cheung, C.M. Che, Chem. Commun. (1996) 1039.